Journal of Catalysis 273 (2010) 59–65

Contents lists available at ScienceDirect

Journal of Catalysis

journal homepage: www.elsevier.com/locate/jcat

Low-temperature hydrocarbon combustion over proton conductor/metal–mixed catalysts

Kota Tsuneyama [a], Shinya Tetanishi [a], Takashi Hibino [a,*], Satoshi Nagao [b], Hirohito Hirata [b], Shin-ichi Matsumoto [b]

[a] *Graduate School of Environmental Studies, Nagoya University, Nagoya, Aichi 464-8601, Japan*
[b] *Higashifuji Technical Center, Toyota Motor Corporation, Susono, Shizuoka 410-1193, Japan*

ARTICLE INFO

Article history:
Received 9 February 2010
Revised 30 April 2010
Accepted 30 April 2010

Keywords:
Hydrocarbon oxidation
Active oxygen
Proton conductor
Electrochemical local cell

ABSTRACT

Catalytic combustion of hydrocarbons is a highly active field of research, particularly in relation to the reduction of pollutant emissions from automobiles. In this study, we report on hydrocarbon oxidation at the internal interfaces of a mixed catalyst consisting of $Sn_{0.9}In_{0.1}P_2O_7$ and Pt powders. In a gaseous mixture of propane, H_2O, and O_2, the H_2O dissociates into protons, electrons and active oxygen species at anodic interface sites, leading to oxidation of the hydrocarbon to CO_2. On the other hand, O_2 reacts with protons and electrons to form H_2O at cathodic interface sites. As a consequence, local electrochemical cells are formed at the interfaces, and undergo self-discharge. It was shown that the mixed catalyst had a high turnover frequency for Pt, yielding high catalytic activity for Pt contents of as low as 0.1 wt% and an initiation temperature for hydrocarbon oxidation of 150 °C.

1. Introduction

Uncombusted hydrocarbons, in addition to CO and NO_x, emitted from gasoline engines are commonly removed by three-way catalysts (TWCs). However, the TWCs available to date require a combustion temperature of 300–500 °C, especially for saturated hydrocarbons, which is much higher than typical exhaust temperatures of <200 °C during cold-start transients. This gap makes it difficult to maintain emission restrictions that are becoming increasingly stringent worldwide, because considerable amounts of hydrocarbons are released into the atmosphere under such low-temperature conditions [1]. Thus, in recent years, there has been increasing interest in low-temperature hydrocarbon combustion as a potential approach to achieve ultra low-emission vehicles [2–5].

The activation of C–H bonds in saturated hydrocarbons is considered to be the key initial step in hydrocarbon oxidation and is accomplished over platinum group metals such as Pt and Pd [6–8]. While the precise nature of the active site is not yet clear, due to the complexity of their operating conditions, there seems to be little doubt regarding the role of chemisorbed or combined oxygen species (so-called active oxygen) in the extraction of hydrogen by breaking of the C–H bond in hydrocarbons [9,10]. In addition, the presence of Ce–Zr–mixed oxides stabilizes the oxidation state of the metal catalyst and therefore, contributes to a reduction in the combustion temperature of the hydrocarbons [11,12]. Although several transition-metal oxides [13] and perovskite-type oxides [14] can also activate O_2 in the gas phase or oxide ions in the lattice due to their redox properties, such oxygen-activating species are not commercially viable for low-temperature hydrocarbon combustion, because of their relatively low levels of activity.

In this study, we focused on H_2O vapor as an active oxygen source and a mixture of proton conductor and electrocatalyst powders as a catalyst. We recently reported that in a proton exchange membrane fuel cell using $Sn_{0.9}In_{0.1}P_2O_7$ and Pt/C as the electrolyte and electrode, respectively, light hydrocarbons, including ethane, propane, and butane, could be directly used as fuels, even in the temperature range of 100–300 °C [15]. More importantly, the hydrocarbons were oxidized to CO_2 with very high faradic efficiency, so that the following reaction proceeded at the Pt/C anode:

$$C_nH_{2n+2} + 2nH_2O \rightarrow nCO_2 + (6n+2)H^+ + (6n+2)e^- \qquad (1)$$

It is known that HO· is formed by the anodic polarization of H_2O [16,17]; therefore, such a radical is likely to be an important active species for breaking the C–H bond in Reaction (1). On the other hand, the following oxygen reduction reaction occurred at the Pt/C cathode as a counter-reaction to Reaction (1):

$$(1.5n+0.5)O_2 + (6n+2)H^+ + (6n+2)e^- \rightarrow (3n+1)H_2O \qquad (2)$$

As a result, the fuel cell exhibited power densities ranging from 10 to 60 mW cm^{-2}, which were dependent on the temperature and the hydrocarbon species.

---

[*] Corresponding author. Fax: +81 52 789 4894.
E-mail address: hibino@urban.env.nagoya-u.ac.jp (T. Hibino).

0021-9517/$ - see front matter © 2010 Elsevier Inc. All rights reserved.
doi:10.1016/j.jcat.2010.04.022

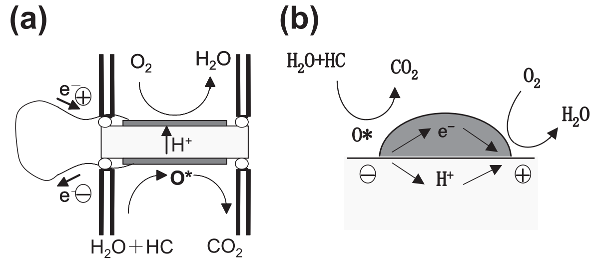

Scheme 1. Schematic illustrations of (a) fuel cell and (b) local electrochemical cell.

Based on these observations, it is expected that an electrochemical reactor for hydrocarbon combustion can be developed through Reactions (1) and (2) at temperatures of 100 °C or higher by short-circuiting the fuel cell, as shown in Scheme 1a. Moreover, if micro-scale electrochemical cells can be successfully produced by mixing the proton conductor powder with the electrocatalyst powder as illustrated in Scheme 1b, then the reaction area for hydrocarbon oxidation can be drastically increased. This paper demonstrates that Reactions (1) and (2) are applicable to hydrocarbon oxidation on solid catalysts, which opens up new possibilities for the development of low-temperature hydrocarbon combustion systems.

2. Experimental

2.1. Materials

$Sn_{0.9}In_{0.1}P_2O_7$ and Pt were used as proton conductor and electrocatalyst, respectively, in the manner previously reported [15]. $Sn_{0.9}In_{0.1}P_2O_7$ was prepared as follows. SnO_2 and In_2O_3 were mixed with H_3PO_4 and ion-exchanged water, and stirred at 300 °C until a high viscosity paste was formed. The paste was calcined in an alumina crucible at 650 °C for 2.5 h, and the product was then ground in a mortar. For electrochemical cell studies, the $Sn_{0.9}In_{0.1}P_2O_7$ powder was uniaxially pressed into pellets (12 mm diameter, ca. 1.5 mm thick) under a pressure of 200 MPa and used as the electrolyte. A Pt/C anode (10 wt% Pt/C, 4.0 mg Pt cm^{-2}) and a Pt/C cathode (10 wt% Pt/C, 0.6 mg Pt cm^{-2}) were purchased from BASF. For catalyst studies, commercially available platinum black was used as a component of the catalyst. The Pt powder was mixed with $Sn_{0.9}In_{0.1}P_2O_7$ and α-Al_2O_3 powders in a mortar for a few minutes. For comparison with the $Sn_{0.9}In_{0.1}P_2O_7$ + Pt-mixed catalyst, a Pt/γ-Al_2O_3 (1 wt% Pt) catalyst, which is used as a standard catalyst at Toyota Motor Corporation, was also tested.

2.2. Electrochemical cell studies

Reactions (1) and (2) were investigated using an electrochemical cell. The two Pt/C electrodes (area: 0.5 cm^2) were attached on opposite sides of the electrolyte without the use of any special binder. In both cases, a Pt mesh was employed as a current collector. (It is reasonable to consider that this mesh does not influence hydrocarbon oxidation because there is a gas diffusion layer between the Pt mesh and Pt/C catalyst layer.) An Au reference electrode was attached to the side surface of the electrolyte. In all experiments except the cyclic voltammetry (CV) measurements, the reference electrode was exposed to atmospheric air. Two gas chambers were set up by placing the cell assembly between two alumina tubes, as illustrated in Fig. 1a. Unless otherwise stated, a mixture of propane and H_2O in Ar (1000 ppm–7% propane and 3% H_2O) was supplied to the anode at a flow rate of 30 mL min^{-1}, and O_2 diluted with Ar (5000 ppm–21% O_2) was supplied to the cathode at a flow rate of 30 mL min^{-1}. The concentrations of propane, COx (CO_2 and CO), and O_2 in the outlet gas from the anode chamber were analyzed using an on-line gas chromatograph. The gas concentrations were obtained after the reaction had achieved a steady state. CV curves were measured between 0 and 1.2 V vs. reversible hydrogen electrode (RHE) at a scan rate of 10 mV s^{-1}. Anodic and cathodic polarization curves were measured by controlling the potential of the working electrode vs. the reference electrode with a potentiostat. Raman analysis was carried out by setting up the electrochemical cell in a spectrophotometer, as shown in Fig. 1b. Raman spectra of the anode surface were recorded during the application of constant current to the electrochemical cell with visible (532 nm) laser excitation. All Raman measurements were conducted at room temperature in air.

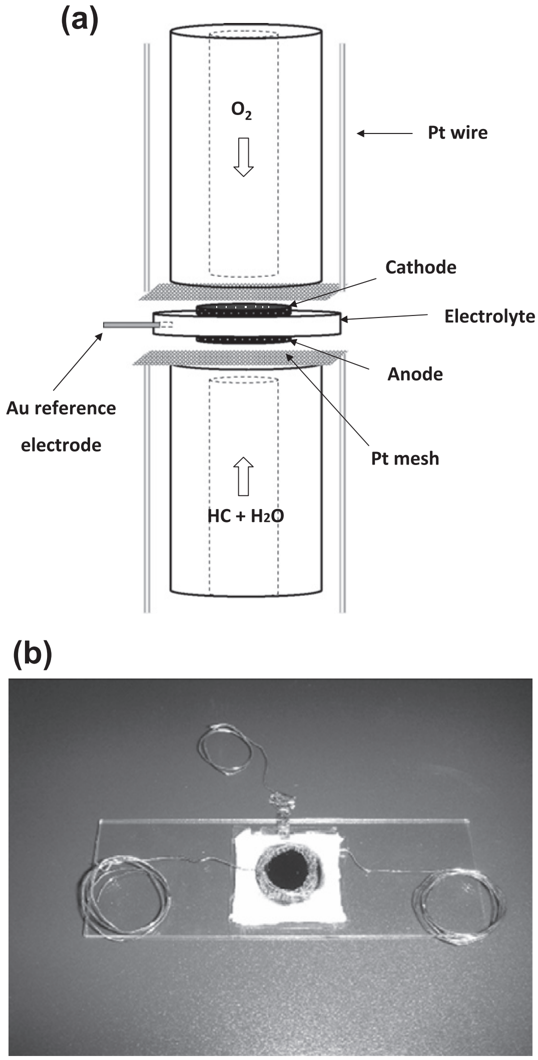

Fig. 1. Electrochemical cells for (a) gas composition, CV, and polarization curve measurements and (b) Raman analysis.

2.3. Catalyst studies

The catalytic activity of the $Sn_{0.9}In_{0.1}P_2O_7$ + Pt-mixed catalyst (0.1–10 wt% Pt) for hydrocarbon oxidation was evaluated under various conditions. The dispersion state of each component in the mixed catalyst was analyzed using scanning electron microscopy (SEM) in conjunction with energy dispersive X-ray (EDX) spectroscopy. The number of reaction sites on the Pt surface was measured by the CO pulse method at room temperature. Catalytic tests were conducted in a fixed-bed flow reactor. Unless otherwise stated, a mixture of 1000 ppm propane, 3% H_2O, and 5000 ppm O_2 in Ar was fed into the reactor, where the space velocity (SV) was in the range of 9500–350,000 h^{-1}. Analysis of the outlet gas was conducted as described earlier. All experiments were performed from room temperature to 600 °C.

3. Results and discussion

3.1. Characterization of active oxygen species

First, the electrochemically produced active oxygen species was characterized. In order to estimate the oxidation ability of the oxygen species, CO_2 production at the Pt/C anode was monitored as a function of oxidation current in the temperature range from room temperature to 300 °C. Fig. 2 shows the CO_2 concentration as a function of current density and includes the theoretical values calculated from Faraday's law. CO_2 was observed as an oxidation product at all temperatures studied. For all current densities, the CO_2 concentrations moved closer to their theoretical values as the temperature was increased. (Small amounts of O_2 and CO were observed as additional products below 200 °C.) In particular, at 200 °C or higher, CO_2 was formed with a current efficiency of approximately 100%, indicating that the oxygen species produced at the Pt/C anode had a very high activity for propane oxidation. In addition, no products were observed under open-circuit conditions even at 300 °C, which indicates that propane is directly converted to CO_2 via Reaction (1).

To gain insight into the active oxygen species, CV measurements were performed at 300 °C. Fig. 3 shows a large anodic peak between +0.3 and +0.7 V (vs. RHE) in both the positive- and negative-direction scans. The presence of these peaks can be interpreted as follows. A Pt–OH species, which is assumed to be active in breaking the C–H bond in propane, is formed between +0.3 and +0.7 V during anodic polarization. Further anodic polarization oxidizes Pt–OH to a PtO species that is assumed to be inactive with respect to the C–H bond and thus, the anodic current drastically decreases at high potentials. On the other hand, cathodic polarization reduces PtO to the Pt–OH species, which again gives rise to a large anodic current due propane oxidation. Therefore, it is suggested that Reaction (1) comprises the following steps.

$$Pt + H_2O \rightarrow Pt - OH + H^+ + e^- \tag{3}$$

$$Pt - OH + (C_3H_8)_{ads} \rightarrow (C_3H_7)_{ads} + H_2O \tag{4}$$

$$(C_3H_7)_{ads} \rightarrow (CH_m)_{ads} + (C_2H_n)_{ads} \tag{5}$$

$$(C_2H_n)_{ads} \rightarrow 2(CH_m)_{ads} \tag{6}$$

$$2Pt - OH + (CH_m)_{ads} \rightarrow CO_2 + Pt + (2 + m)H^+ + (2 + m)e^- \tag{7}$$

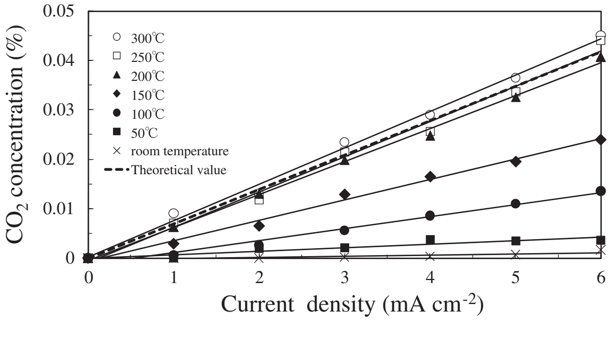

Fig. 2. CO_2 formation at the Pt/C working electrode in a propane–H_2O feed mixture from room temperature to 300 °C. Theoretical values calculated from Faraday's law are also included. At temperatures below 200 °C, small amounts of O_2 and CO were formed in addition to CO_2.

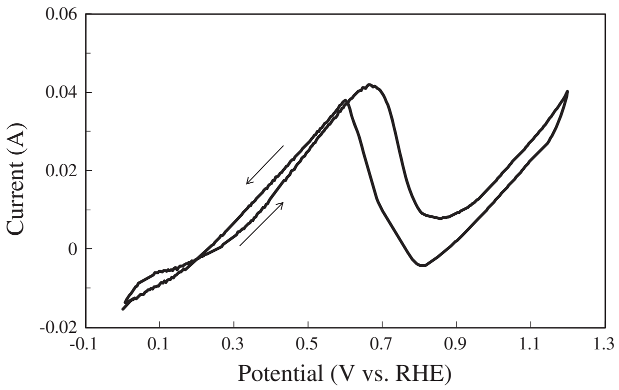

Fig. 3. CV profile for the Pt/C working electrode in a propane–H_2O feed mixture at 300 °C. While the Pt/C counter electrode was exposed to ambient atmosphere, the Au reference electrode was supplied with hydrogen.

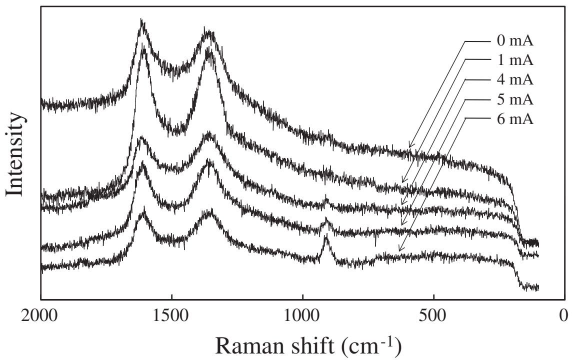

Fig. 4. Raman spectra of the Pt/C working electrode at room temperature. Constant currents were applied to the electrochemical cell under ambient atmosphere. Peaks observed at 1360 and 1600 cm^{-1} are assigned to amorphous carbon and crystalline graphite, respectively.

A similar mechanism was proposed by Brummer et al. [18]. Raman spectra measured in the range of 100–2000 cm^{-1} with varying current through the Pt/C electrode provide evidence for this mechanism. As can be seen in Fig. 4, a band appears at 918 cm^{-1} when current is flowing, which is assigned to the Pt–OH bending mode [19]. (This is supported by the fact that a similar band was observed when only Pt was used as the electrode.) It is thus reasonable to conclude that the active oxygen species for propane oxidation is OH· combined with Pt.

3.2. Electrochemical testing of Scheme 1

The method of oxidation of hydrocarbons represented in Scheme 1a was first investigated using several electrochemical techniques. It is necessary to generate a large electromotive force (EMF) and short-circuit current in the fuel cell, even if the hydrocarbon and O_2 concentrations are at ppm levels. Fuel-cell tests were performed at 300 °C using propane and O_2 with various concentrations. Fig. 5a shows that although the cell performance decreased with propane concentration, an EMF of 463 mV and a short-circuit current of 28 mA cm^{-2} could be obtained at a propane concentration of 1000 ppm. Fig. 5b shows a more surprising result in that the fuel cell still achieved an EMF of 332 mV and a short-circuit current of 17 mA cm^{-2} when the O_2 concentration was decreased to the stoichiometric value of 5000 ppm required for the combustion of 1000 ppm propane. These results at least

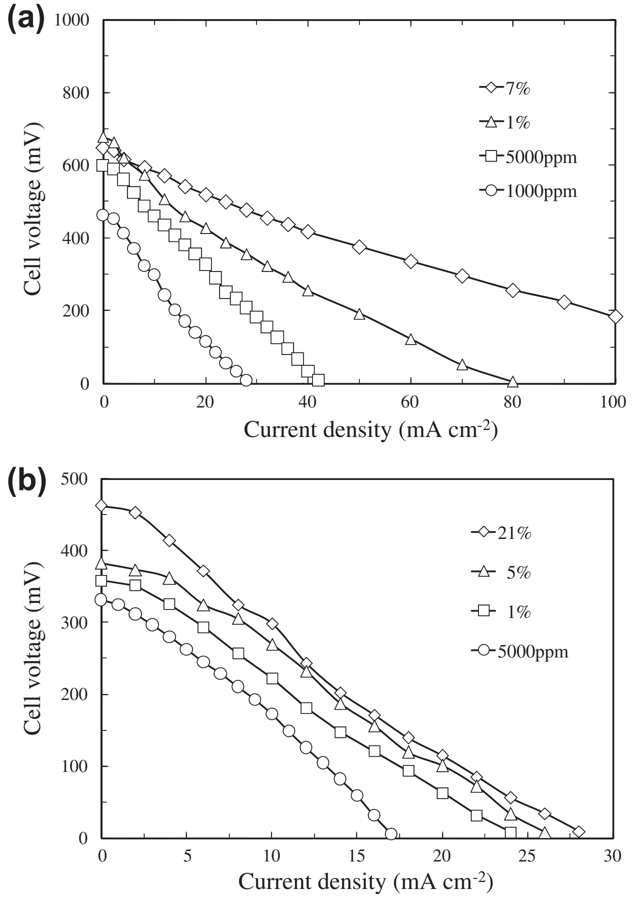

Fig. 5. Fuel-cell performance at 300 °C using (a) propane and (b) O_2 with various concentrations. The fuel-cell tests were conducted using the four-prove method, where the voltage drop due to Pt lead wires could be eliminated.

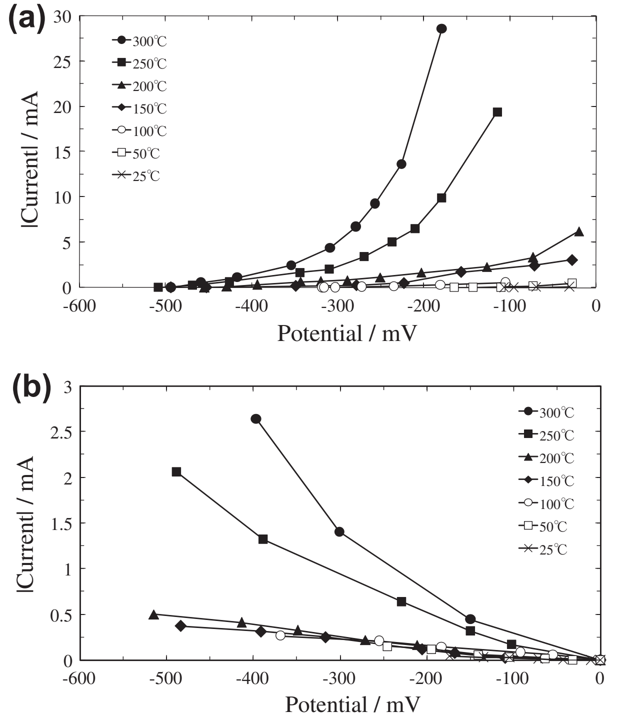

Fig. 6. Polarization curves from room temperature to 300 °C observed for the Pt/C working electrode in (a) a mixture of 1000 ppm propane and 3% H_2O in Ar and (b) 5000 ppm O_2 diluted with Ar. Both the Pt/C counter and Au reference electrodes were exposed to ambient atmosphere.

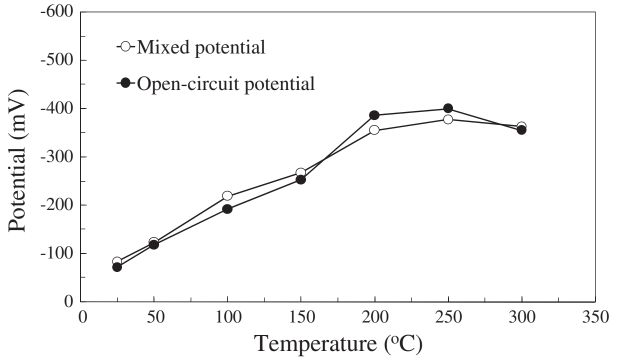

Fig. 7. Mixed potential estimated from the intersection points of the anodic and cathodic polarization curves and open-circuit potentials of the Pt/C working electrode. The open-circuit potentials were obtained in a mixture of 1000 ppm propane, 3% H_2O, and 5000 ppm O_2.

suggest the possibility of a fuel-cell type of reactor capable of operating at low propane and O_2 concentrations.

Assuming that Scheme 1a can be represented by the reaction pathways shown in Scheme 1b, then propane is oxidized to CO_2 through Reaction (1) at anodic sites on the Pt/C electrode, giving rise to a negative potential due to rich electrons. On the other hand, oxygen is reduced to H_2O through Reaction (2) at cathodic sites on the same Pt/C electrode, giving rise to a positive potential due to poor electrons. (The appearance of the anode and cathode sites on the Pt particle is thought to be due to the heterogeneity of the Pt surface, which results from the difference in the atomic lattice and structure defects.) As a result, a local galvanic cell is formed at the same Pt/C electrode. Since the electrode also functions as a lead wire, the cell becomes short-circuited. In this case, the rates of Reactions (1) and (2) are equal, resulting in the appearance of a mixed potential on the Pt/C electrode. A similar phenomenon has been reported in various gas mixtures used in potentiometric gas sensors [20,21]. In order to verify this assumption, the mixed potentials were estimated from the polarization curves for propane oxidation according to Reaction (1) and for oxygen reduction according to Reaction (2), and then compared with the open-circuit potentials for the Pt/C electrode in a feed mixture of propane, H_2O, and O_2. Fig. 6a and b displays the anodic polarization curves for a mixture of 1000 ppm propane and 3% H_2O in Ar and the cathodic polarization curves for 5000 ppm O_2 in Ar, respectively, from room temperature to 300 °C. The intersection points of the anodic and cathodic polarization curves, which correspond to the mixed potentials, are plotted in Fig. 7. On the other hand, the open-circuit potential of the Pt/C electrode was measured in a mixture of 1000 ppm propane, 3% H_2O, and 5000 ppm O_2 from room temperature to 300 °C. These results are also included in Fig. 7. The mixed potential values are almost in agreement with the open-circuit potential values, which demonstrates that Reactions (1) and (2) do occur at the Pt/C electrode according to Scheme 1b. Moreover, we observed CO_2 in the outlet gas from the Pt/C electrode when the open-circuit potential was measured at 250 °C. Interestingly, the short-circuit current value calculated from the CO_2 concentration was approximately 1.3 mA, which is roughly in agreement with the value of 1.5 mA estimated from the intersection points of the polarization curves, which provides further evidence for the above assumption.

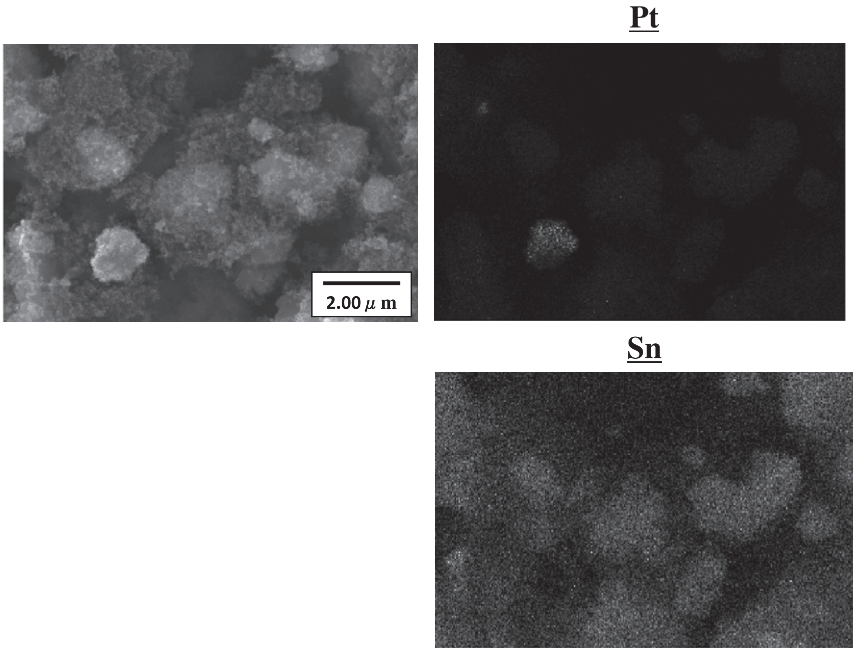

Fig. 8. SEM and EDX characterizations of the $Sn_{0.9}In_{0.1}P_2O_7$ + Pt mixed catalyst.

3.3. Hydrocarbon oxidation over $Sn_{0.9}In_{0.1}P_2O_7$ + Pt-mixed powders

Scheme 1b allows for the spontaneous formation of the Pt–OH species and the subsequent oxidation of propane in a propane, H_2O, and O_2 mixture. However, the electrochemical cell inherently has a much smaller reaction area than conventional solid catalysts. Therefore, an attempt was made to increase the reaction area for hydrocarbon oxidation by mixing the $Sn_{0.9}In_{0.1}P_2O_7$ and Pt powders. Fig. 8 shows the results of SEM and EDX analysis of the mixed catalyst. It can be seen that Pt aggregates, several microns in size, are interspersed between the $Sn_{0.9}In_{0.1}P_2O_7$ particles.

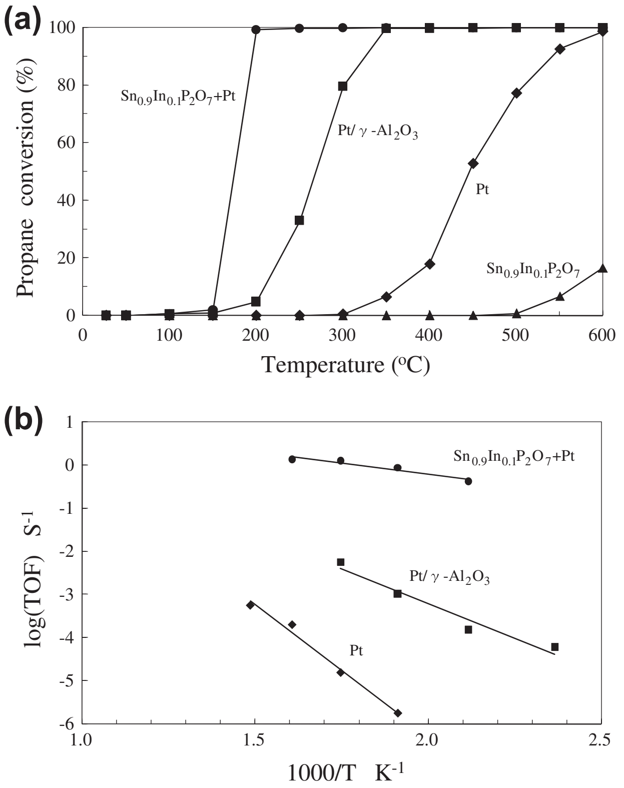

Fig. 9. Catalytic activity of various catalysts for propane oxidation from room temperature to 600 °C. (a) Propane conversion for $Sn_{0.9}In_{0.1}P_2O_7$ + Pt (1 wt% Pt), $Sn_{0.9}In_{0.1}P_2O_7$, Pt (10 mg), and Pt/γ-Al_2O_3 (1 wt% Pt) catalysts. A constant SV of 9500 h^{-1} was maintained by controlling the amount of α-Al_2O_3 additives. (b) TOF for $Sn_{0.9}In_{0.1}P_2O_7$ + Pt (1 wt% Pt), Pt (10 mg), and Pt/γ-Al_2O_3 (1 wt% Pt) catalysts. The number of reaction sites on the Pt surface was measured by the CO pulse method at room temperature.

The activity of the $Sn_{0.9}In_{0.1}P_2O_7$ + Pt-mixed catalyst for hydrocarbon oxidation was measured in a feed mixture of propane, H_2O, and O_2 in Ar. Fig. 9a shows the temperature dependence of the propane conversion for the $Sn_{0.9}In_{0.1}P_2O_7$ + Pt-mixed catalyst (1 wt% Pt) and the individual components $Sn_{0.9}In_{0.1}P_2O_7$ and Pt. For comparison, data for a Pt/γ-Al_2O_3 catalyst (1 wt% Pt) is also shown. While the reaction initiation temperatures for the $Sn_{0.9}In_{0.1}P_2O_7$ and Pt catalysts were 550 and 350 °C, respectively, the initiation temperature for the $Sn_{0.9}In_{0.1}P_2O_7$ + Pt-mixed catalyst was drastically reduced to 150 °C, which is lower than the initiation temperature of 200 °C for the Pt/γ-Al_2O_3 catalyst. Even larger differences were observed in the temperature at which 90% conversion was achieved (defined as $T_{90\%}$); $T_{90\%}$ was approximately 175 °C for $Sn_{0.9}In_{0.1}P_2O_7$ + Pt, 330 °C for Pt/γ-Al_2O_3, and 525 °C for Pt. ($T_{90\%}$ for $Sn_{0.9}In_{0.1}P_2O_7$ could not be determined within the temperature range tested.) The temperature dependence of the turnover frequency (TOF) for Pt in the above catalysts is shown in Fig. 9b. It can be seen that the TOF for the $Sn_{0.9}In_{0.1}P_2O_7$ + Pt-mixed catalyst is two to four orders of magnitude higher than that for the Pt/γ-Al_2O_3 catalyst in the tested temperature range. Moreover, the $Sn_{0.9}In_{0.1}P_2O_7$ + Pt-mixed catalyst showed a considerably lower activation energy (19.6 kJ mol^{-1}) than the Pt/γ-Al_2O_3 catalyst (61.9 kJ mol^{-1}). Therefore, it can be concluded that the $Sn_{0.9}In_{0.1}P_2O_7$ + Pt-mixed catalyst produces a highly active oxygen species for propane oxidation. In addition, it is demonstrated that the formation of such an active oxygen species is first accomplished by combining $Sn_{0.9}In_{0.1}P_2O_7$ and Pt in a similar manner to the case of the electrochemical cell.

The effect of varying the Pt content in the mixed catalyst on its catalytic activity was also investigated. Fig. 10 shows the propane conversion as a function of temperature for the $Sn_{0.9}In_{0.1}P_2O_7$ + Pt-mixed catalyst with different Pt wt%. Again, data for the Pt/γ-Al_2O_3 catalyst (1 wt% Pt) are included for comparison. At a temperature

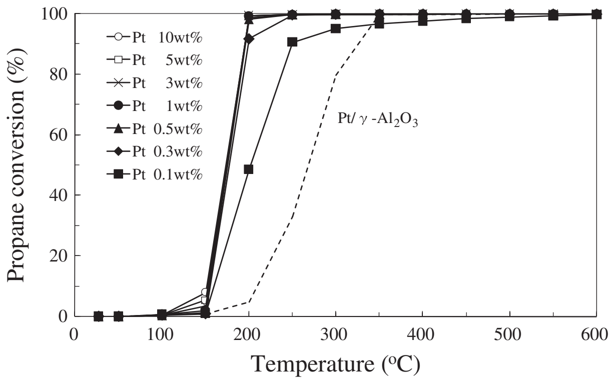

Fig. 10. Catalytic activity of the $Sn_{0.9}In_{0.1}P_2O_7$ + Pt-mixed catalyst with various Pt contents for propane oxidation. The experimental conditions used are the same as in Fig. 9a.

of 200 °C, approximately 100% propane conversion was achieved for Pt contents of >0.5 wt%. However, at 250 °C, the propane conversion was approximately 90% even for 0.1 wt% Pt, which is higher than the value of 35% for the Pt/γ-Al_2O_3 catalyst. Considering the very poor level of Pt dispersion in the mixed catalyst, it is remarkable to observe such high catalytic activity for 0.1 wt% Pt, since catalytic activity is thought to be determined by the production of highly oxidizing OH· radicals at the $Sn_{0.9}In_{0.1}P_2O_7$/Pt interfaces.

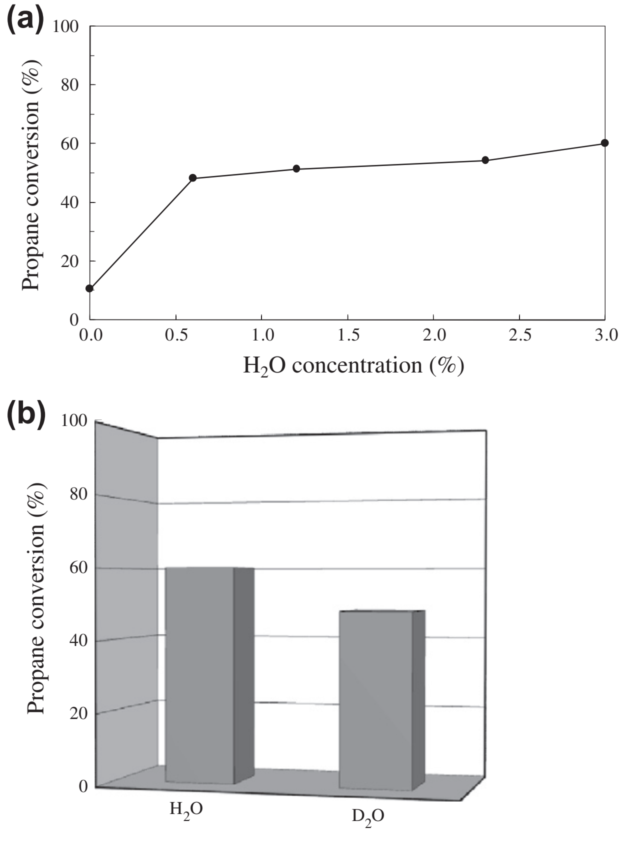

Fig. 11. Catalytic properties of the $Sn_{0.9}In_{0.1}P_2O_7$ + Pt-mixed catalyst for propane oxidation under various conditions. (a) Influence of H_2O concentration on propane conversion at 200 °C with a SV of 64,000 h^{-1}. The propane and O_2 concentrations were kept constant at 1000 and 5000 ppm, respectively. H_2O concentration was measured using a dew-point hygrometer. (b) H/D isotope effect on propane conversion at 200 °C with a SV of 64,000 h^{-1} in a mixture of 3% H_2O or 3% D_2O, 1000 ppm propane, and 5000 ppm O_2.

The dependence of the propane conversion on the H_2O concentration in the reactant gas was next investigated. As shown in Fig. 11a, the propane conversion at 200 °C increased with increasing H_2O concentration, possibly due to an increase in the rate of Reaction (1). Another possibility is that proton migration through the bulk $Sn_{0.9}In_{0.1}P_2O_7$ (see Scheme 1b) is enhanced with increasing H_2O concentration. For example, proton conductivity in $Sn_{0.9}In_{0.1}P_2O_7$ at 250 °C has been measured to be 0.19, 0.20, and 0.22 S cm^{-1} at H_2O concentrations of 0.6%, 3%, and 10%, respectively [22,23]. To clarify this, the H/D isotope effect on the activity of the mixed catalyst was investigated, because the electrical resistance of proton conductors commonly increases when protons are replaced with deuterons [24]. As shown in Fig. 11b, propane conversion at 200 °C was reduced when H_2O vapor was replaced with D_2O vapor, which indicates that proton conduction in $Sn_{0.9}In_{0.1}P_2O_7$ is a contributing factor to the high propane conversion at low temperatures. However, there may still be other factors that play important roles in propane oxidation. It has been proposed that some acidic catalyst supports can effectively promote hydrocarbon oxidation over Pt [25]. Although $Sn_{0.9}In_{0.1}P_2O_7$ is also a solid acid, its specific surface area is less than 0.5 $m^2\ g^{-1}$, which may be too small to enhance the catalytic activity of the weakly dispersed Pt.

The $Sn_{0.9}In_{0.1}P_2O_7$ + Pt-mixed catalyst also exhibited the following important characteristics:

(1) Similarly high catalytic activities were obtained for other saturated hydrocarbons; $T_{90\%}$ was 290 °C for ethane and 200 °C for butane (Fig. S1).
(2) Negative effects on propane oxidation due to the presence of CO and NO were relatively small; $T_{90\%}$ was 240 °C with 1% CO and 300 °C with 1000 ppm NO (Fig. S2).
(3) The influence of the SV on propane conversion was not significant (Fig. S3).
(4) The catalytic activity of the $Sn_{0.9}In_{0.1}P_2O_7$ + Pt-mixed catalyst showed a higher catalytic activity than that of Pt/γ-Al_2O_3 + Rh/CeO_2-mixed catalyst (Fig. S4).

Based on these results, this mixed catalyst is a promising candidate material for low-temperature hydrocarbon combustion. However, there is still the need for expensive Pt, although only at 0.1 wt%, to achieve high activity for hydrocarbon oxidation. As has been pointed out, Pt dispersion in the mixed catalyst was very low, which suggests that if smaller Pt particles were deposited on the $Sn_{0.9}In_{0.1}P_2O_7$ surface by impregnation of various precursors such as $H_2PtCl_6{\cdot}6H_2O$ and $Pt(NH_3)_4Cl_2{\cdot}H_2O$, the degree of Pt utilization could be significantly enhanced. Replacing Pt with metal carbides [26], metal oxynitrides [27], or transition-metal macrocycles [28] may also be possible, because these materials have been reported as potential anode or cathode catalysts in low-temperature fuel cells.

4. Conclusions

This study proposed a method for the production of an active oxygen species from H_2O vapor at the proton conductor–electrocatalyst interface and investigated the use of this active oxygen for low-temperature hydrocarbon combustion. $Sn_{0.9}In_{0.1}P_2O_7$ and Pt were used as the proton conductor and electrocatalyst, respectively. Propane was oxidized to CO_2 during discharge at room temperature or higher, and the CO_2 formation rate achieved the theoretical value based on Faraday's law at 200 °C. CV measurements confirmed the formation of an active oxygen species over the Pt for certain electrode potentials, and Raman analysis indicated that this species was an OH· radical. The electrochemical activation of oxygen also occurred under open-circuit conditions when both H_2O and O_2 were present in the reaction system, which is interpreted as a mixed potential mechanism. This phenomenon was then applied to a $Sn_{0.9}In_{0.1}P_2O_7$ + Pt mixed catalyst. Compared with a Pt/γ-Al_2O_3 catalyst, the mixed catalyst showed significantly larger TOF values for Pt, thus providing higher catalytic activity at low temperatures and smaller quantities of Pt.

Appendix A. Supplementary material

Supplementary data associated with this article can be found, in the online version, at doi:10.1016/j.jcat.2010.04.022.

References

[1] M.V. Twigg, Appl. Catal. B 70 (2007) 2.
[2] R. Schneider, D. Kieβling, G. Wendt, Appl. Catal. B 28 (2000) 187.
[3] L. Li, J. Chen, S. Zhang, N. Guan, M. Richter, R. Eckelt, R. Fricke, J. Catal. 228 (2004) 12.
[4] S. Sharma, M.S. Hegde, Catal. Lett. 112 (2006) 69.
[5] T.F. Garetto, E. Rincon, C.R. Apesteguia, Appl. Catal. B 73 (2007) 65.
[6] R. Burch, D.J. Crittle, M.J. Hayes, Catal. Today 47 (1999) 229.
[7] T.F. Garetto, C.R. Apesteguía, Catal. Today 62 (2000) 189.
[8] J.Y. Luo, M. Meng, J.S. Yao, X.G. Li, Y.Q. Zha, X. Wang, T.Y. Zhang, Appl. Catal. B 87 (2009) 92.
[9] Y. Yazawa, H. Yoshida, N. Takagi, S. Komai, A. Satsuma, T. Hattori, J. Catal. 187 (1999) 15.
[10] B. Grbic, N. Radic, B. Markovic, P. Stefanov, D. Stoychev, Ts. Marinova, Appl. Catal. B 64 (2006) 51.
[11] J.R. González-Velasco, M.A. Gutiérrez-Ortiz, J-L. Marc, J.A. Botas, M.P. González-Marcos, G. Blanchard, Appl. Catal. B 22 (1999) 167.
[12] A. Hartridge, A.K. Bhattacharya, J. Phys. Chem. Solids 63 (2002) 441.
[13] A. Cimino, F.S. Stone, Adv. Catal. 47 (2002) 141.
[14] H. He, H.X. Dai, C.T. Au, Appl. Catal. B 33 (2001) 65.
[15] P. Heo, K. Ito, A. Tomita, T. Hibino, Angew. Chem. Int. Ed. 47 (2008) 7841.
[16] N.M. Markovic, P.N. Ross, Surf. Sci. Rep. 45 (2002) 117.
[17] W.S. Li, D.S. Lu, J.L. Luo, K.T. Chuang, J. Power Sources 145 (2005) 376.
[18] B. Brummer, J.I. Ford, M.J. Turner, J. Phys. Chem. 69 (1965) 3424.
[19] K. Bedürftig, S. Völkening, Y. Wang, J. Wintterlin, K. Jacobi, G. Ertl, J. Chem. Phys. 111 (1999) 11147.
[20] N. Miura, G. Lu, N. Yamazoe, H. Kurosawa, M. Hasei, J. Electrochem. Soc. 143 (1996) L33.
[21] F.H. Garzon, R. Mukundan, E.L. Brosha, Solid State Ionics 136–137 (2000) 633.
[22] M. Nagao, A. Takeuchi, P. Heo, T. Hibino, M. Sano, A. Tomita, Electrochem. Solid-State Lett. 9 (2006) A105.
[23] M. Nagao, T. Kamiya, P. Heo, A. Tomita, T. Hibino, M. Sano, J. Electrochem. Soc. 153 (2006) A1604.
[24] T. Norby, Solid State Ionics 40–41 (1990) 857.
[25] S. Sharma, M.S. Hegde, R.N. Das, M. Pandey, Appl. Catal. A 337 (2008) 130.
[26] P. Heo, M. Nagao, M. Sano, T. Hibino, J. Electrochem. Soc. 154 (2007) B53.
[27] A. Takagaki, Y. Takahashi, F. Yin, K. Takanabe, J. Kubota, K. Domen, J. Electrochem. Soc. 156 (2009) B811.
[28] M. Lefevre, J.P. Dodelet, Electrochim. Acta 48 (2003) 2749.